Dynamics of overheated relativistic bubbles

Author: Marc Romeu Casas
Facultat de Física, Universitat de Barcelona, Diagonal 645, 08028 Barcelona, Spain.

Advisor: Jorge Casalderrey Solana

Abstract: In this work we study the dynamics of overheated expanding relativistic bubbles in the context of first order phase transitions. Contrary to overcooled bubbles, these have been poorly studied. We use a simplified equation of state and determine the different kind of expanding regimes. We find three possible regimes: deflagration, detonation and hybrids. For each of these regimes, we compute the velocity and enthalpy profiles and find qualitative differences between the dynamics of overcooled and overheated bubbles.

I. INTRODUCTION

The hydrodynamics of overcooled relativistic bubbles has been studied in the context of cosmological first order phase transitions (FOPT) [1–4] such as electroweak and quark-hadron phase transitions. As the universe slowly expanded and cooled, matter in the early universe could have cooled past the phase transition point and enter into a hot metastable state. Eventually, with the nucleation of bubbles, the transition to the cold stable state occurs. These bubbles expand and collide, producing gravitational waves that could potentially be detected.

Another context where FOPT are important is neutron star (NS) mergers. Before the collision, matter is in the cold phase of quantum chromodynamics (QCD), and heats up during the collision. This process is slow enough to turn matter into a metastable state of overheated hadronic phase. Then, matter could decay to the preferred hot deconfined phase via bubble nucleation. These FOPT take place in the opposite direction of the cosmological ones.

These collisions could produce Mega-Hertz gravitational waves so they may give information about the quantum chromodynamics interacting matter in presence of a strong gravitational field [5]. For this reason, it's interesting to know and characterize the profiles of these bubbles.

While the dynamics of overcooled bubbles has been extensively studied, little is known about overheated relativistic bubbles. In this thesis, we present the first hydrodynamic study of these bubbles, which could emerge from cold to hot FOPT.

Natural units are used in this study ($c = \hbar = 1$).

II. EQUATIONS OF STATE AND BUBBLE NUCLEATION

In this first exploratory study we use a simplified equation of state (EoS). Both phases are described with the EoS of a relativistic gas. The only difference is that in the EoS of the hadronic phase, we need to include the self-interaction potential $\epsilon > 0$. Having these two requirements, we model the EoS of the hadronic phase as

$$p_h = \frac{1}{3}a_h T^4 + \epsilon \qquad e_h = a_h T^4 - \epsilon \tag{1}$$

and in the quark phase

$$p_q = \frac{1}{3}a_q T^4 \qquad e_q = a_q T^4 \tag{2}$$

where $a_q \neq a_h$ depends on the number of bosons and fermions that are in the plasma. a_q and a_h don't need to be specified for computing v and w profiles. Adding both quantities gives us the enthalpy ($w = e + p$)

$$w_q = \frac{4}{3}a_q T^4 \qquad w_h = \frac{4}{3}a_h T^4 \tag{3}$$

From EoS (1) and (2) we obtain the constant value for the speed of sound $c_s^2 = dp/de = 1/3$. Before the bubble was nucleated, the matter was in a metastable hadronic phase with enthalpy w_N.

We consider now that there is a spherically symmetric bubble nucleated in the quark phase inside a region of hadronic phase. This bubble has been expanding for enough time with constant velocity v_w so that it has radius $R_\mathrm{bubble} = v_\mathrm{w}\, t$, where t is the elapsed time from the nucleation. Far from the wall, we have that matter in both phases is at rest. To guarantee this, the time elapsed has to be large enough to ensure that inside the bubble, far from the wall, the initial fluctuation disappeared and the matter is at rest. Outside the bubble, the matter was already at rest before bubble nucleation. Only solutions from which the velocity reaches zero at both sides of the wall are compatible with these assumptions. To find the enthalpy and velocity profiles, we can apply hydrodynamic equations when the velocity gradients are small enough.

To ensure that the bubble is expanding, the pressure inside the bubble must be larger than the pressure on the outside. This implies that the enthalpy of the quark region must be larger than the hadronic one. Before the nucleation of the bubble occurred, all the plasma was in equilibrium in the hadronic phase with a constant energy density. After the nucleation, outside and far from the

bubble wall, the energy density has not changed and, inside the bubble (far from the wall), the matter in the hot phase has higher energy density. This implies that the energy density in the surroundings of the wall is lower than the nucleation energy outside and far from the wall, so the energy is conserved. The fact that the energy density inside the bubble is higher than on the outside implies that the velocity of the matter in the surroundings of the wall must go towards the inside of the bubble. We choose the inflowing velocity field to be negative ($v < 0$). This is opposite to what we have in cosmological phase transitions, where energy outside the bubble is greater than inside, so the fluid must go from the inside to the outside of the bubble ($v > 0$).

III. HYDRODYNAMIC EQUATIONS

To describe the hydrodynamics of the bubbles, we assume that the matter can be described as a perfect fluid. This implies that the energy-momentum tensor is $T_{\mu\nu} = w\, u_\mu\, u_\nu - g_{\mu\nu} p$, with w and p being the enthalpy and pressure of the matter, respectively. We assume that there is an expanding bubble of quark matter (subindex q) with spherical symmetry in a medium of hadronic matter (subindex h). The interphase wall has constant velocity $0 < v_\mathrm{w} < 1$ in the rest frame of the centre of the bubble.

The evolution equations of the system can be obtained starting with the conservation condition $\partial_\mu T^{\mu\nu} = 0$ with spherical symmetry. A detailed derivation of the procedure required to obtain these equations can be found in [1, 3]. As a result, we get two ODE: the first gives the fluid velocity v in the rest frame of the centre of the bubble, which can be integrated independently; the second one gives the enthalpy w. Using the assumption that the bubble is expanding with constant velocity v_w, the hydrodynamic profile becomes self-similar. Both equations can be written with respect to the dimensionless parameter $\xi = r/t$ (with r being the radial coordinate representing the distance from the centre of the bubble and t, the time elapsed from the nucleation of the bubble). This implies that the profiles do not change its shape and each point in a radius r is expanding with the same velocity ξ with respect to the centre of the bubble. As consequence, the quark phase becomes bigger as time passes, and eventually could merge with other bubbles resulting in a entire region of quark phase. The equations are

$$\frac{dv}{d\xi} = \frac{2v}{\xi(1-\xi v)\gamma^2}\left(\frac{\mu^2}{c_s^2} - 1\right)^{-1} \tag{4}$$

$$\frac{dw}{d\xi} = w\left(1 + \frac{1}{c_s^2}\right)\gamma^2 \mu \frac{dv}{d\xi} \tag{5}$$

where $\gamma(v) = 1/\sqrt{1-v^2}$ is the Lorentz factor and $\mu(\xi, v) = \frac{\xi - v}{1-\xi v}$, the Lorentz-tranformed velocity v in the local rest frame expanding with velocity ξ. We can integrate these two equations and obtain the fluid profile if we specify the initial conditions. Figure 1 shows different solutions for the equation (4) for $v < 0$. This condition on v is necessary to obtain solutions that fulfill the desired equations of state. In this picture it has also been included several relevant conditions for the discussion of the possible physical solutions.

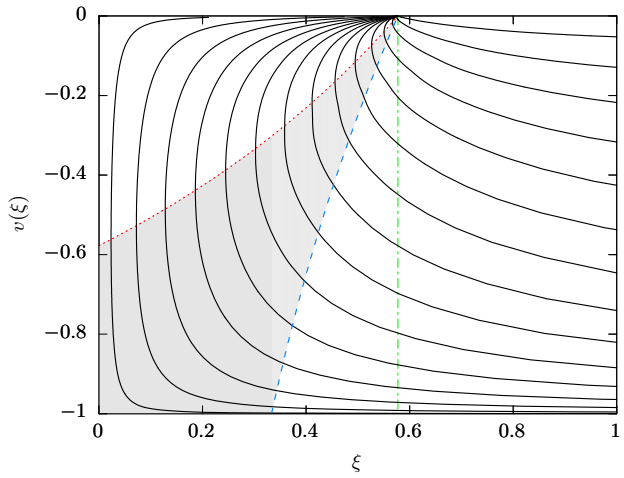

Figure 1. Solution curves of the ODE in (4) with several initial conditions. The red dotted line represents the point where velocity in the RF of the wall equals the speed of sound ($\mu(\xi, v) = c_s$). The blue dashed line represents the points where the shock front ends ($\mu(\xi, v)\xi = c_s^2$). The green dotted-dashed line represents $\xi = c_s$. Shadowed region is not allowed as explained in section V A.

Figure 1 gives the key information to determine the possible kinds of solutions that could exist. There are two ways to build solutions which fulfill that the velocities on both sides of the wall go to zero. The first one is that the velocity profile evolves to zero smoothly. This is only possible if the solution lies on the top left side of Figure 1. The second possibility is through a discontinuity in the profile that fulfills the energy conservation conditions. There are two different kinds of discontinuities, bubble walls, where the phase changes, and shocks, where the phase is the same in both sides. Bubble wall velocity depends on microscopic velocities of the matter in the bubble and cannot be determined without resorting to microscopic calculations. The velocity of the shock is determined by hydrodynamics. There is no possibility of connecting smoothly to zero neither when $\xi \to 0$ (interior of the wall) or when $\xi \to 1$ (exterior of the wall), consequently, discontinuities are necessary to meet the physical requirements.

In this work, we use two different rest frames (RF). The first one is the most natural one, the RF of the centre of the bubble. Velocities in this RF are denoted with no distinction (v), as done in equations (4) and (5). The other RF is the local one of a specific velocity ξ, whose velocities are denoted with a tilde ($\tilde{v}$). Figure 2 shows our conventions for positive velocities in both RF. The

left hand side of each picture represents the quark matter bubble and the right hand side, the outside with hadronic matter.

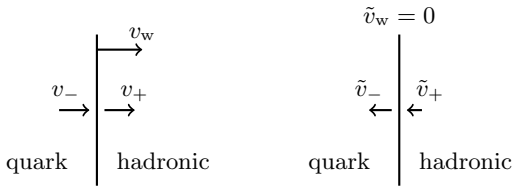

Figure 2. Notation and positive definitions for velocities in both RF. The diagram on the left represents the centre of bubble RF, where the velocity of the wall is defined. The diagram on the right represents the wall RF, where the velocity of the wall is zero.

We can transform the velocities from one RF into the other using the function $\mu(\xi, v)$. The velocity in the local RF of some velocity ξ is $\tilde{v} = \mu(\xi, v)$. With our choose of signs it also holds that $v = \mu(\xi, \tilde{v})$.

IV. RELATIONS OF HYDRODYNAMIC DISCONTINUITIES

Integrating the same conservation equation ($\partial_\mu T^{\mu\nu} = 0$) across the wall, we can get the following equations that relate the properties of the matter in front (+) and behind (-) the wall in the RF of the wall:

$$w_+ \tilde{v}_+^2 \gamma_+^2 + p_+ = w_- \tilde{v}_-^2 \gamma_-^2 + p_- \tag{6}$$

$$w_+ \tilde{v}_+ \gamma_+^2 = w_- \tilde{v}_- \gamma_-^2. \tag{7}$$

We can insert the EoS (1) and (2) in the equation (6) to get another matching condition (MC) that only depends on w and v at both sides of the wall (equation (7) already fulfills this). The matter behind the wall belongs to the quark phase and the matter in front of the wall, to the hadronic phase. This leaves us with

$$w_+(\tilde{v}_+^2 \gamma_+^2 + \frac{1}{4}) + \epsilon = w_-(\tilde{v}_-^2 \gamma_-^2 + \frac{1}{4}) \tag{8}$$

Relations (7) and (8) give us how w and v are related behind and in front of the wall. We refer to these two equations as matching conditions (MC). These are very important because it allows us to build profiles that reach $v = 0$ in regions where the evolution of the equation (4) do not go to zero smoothly. Shocks (discontinuities in the same phase) follow the same equations but setting the value of $\epsilon = 0$.

Equations (7) and (8) can be solved for $\tilde{v}_+$ and $\tilde{v}_-$ using $\alpha_+ = \frac{4\epsilon}{3w_+}$ as a parameter to see the possible region where solutions of the matching conditions exist. These can be seen in Figure 3. The MC of a shock corresponds to setting the parameter $\alpha_+ = 0$ which gives us the condition $\tilde{v}_+ \tilde{v}_- = c_s^2$. This condition in represented in Figures 1 and 3 with a blue dashed line.

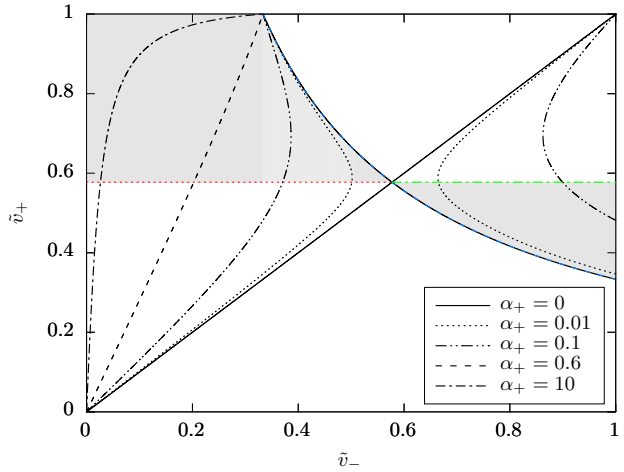

Figure 3. Matching conditions solutions for $\tilde{v}_+$ and $\tilde{v}_-$ using α_+ as a parameter.

It is known from the studies of hydrodynamics that only regions where both $\tilde{v}_+$ and $\tilde{v}_-$ are either supersonic or subsonic are allowed. This is necessary to ensure that the entropy inside the bubble is larger than in the outside. A detailed discussion can be found in [6]. For this reason, the MC solutions that do not hold these conditions are shadowed.

In Figure 3, the three coloured lines correspond to the limits of the regions where the result of solving the MC gives a physical profile that fulfills the mentioned entropy conditions. These three lines can be represented in Figure 1 using Lorentz transformation and assuming that one of the velocities of the discontinuity is zero in the RF of the centre of the bubble ($v_- = 0$ for deflagration and $v_+ = 0$ for detonations).

The upper left region in Figure 3 corresponds to the shadowed region in Figure 1. The bottom right region also corresponds to the region in Figure 1 between the blue and the green lines. Unlike the former case, this region is not shadowed in this figure, because it exist as a hybrid solution, as explained in section V C.

In the following section, the possible profiles are discussed. To get a solution, we need to specify only two parameters: v_w and ϵ. For each profile, the quantity $r = w_-/w_+$, which measures the energy jump across the wall, is computed.

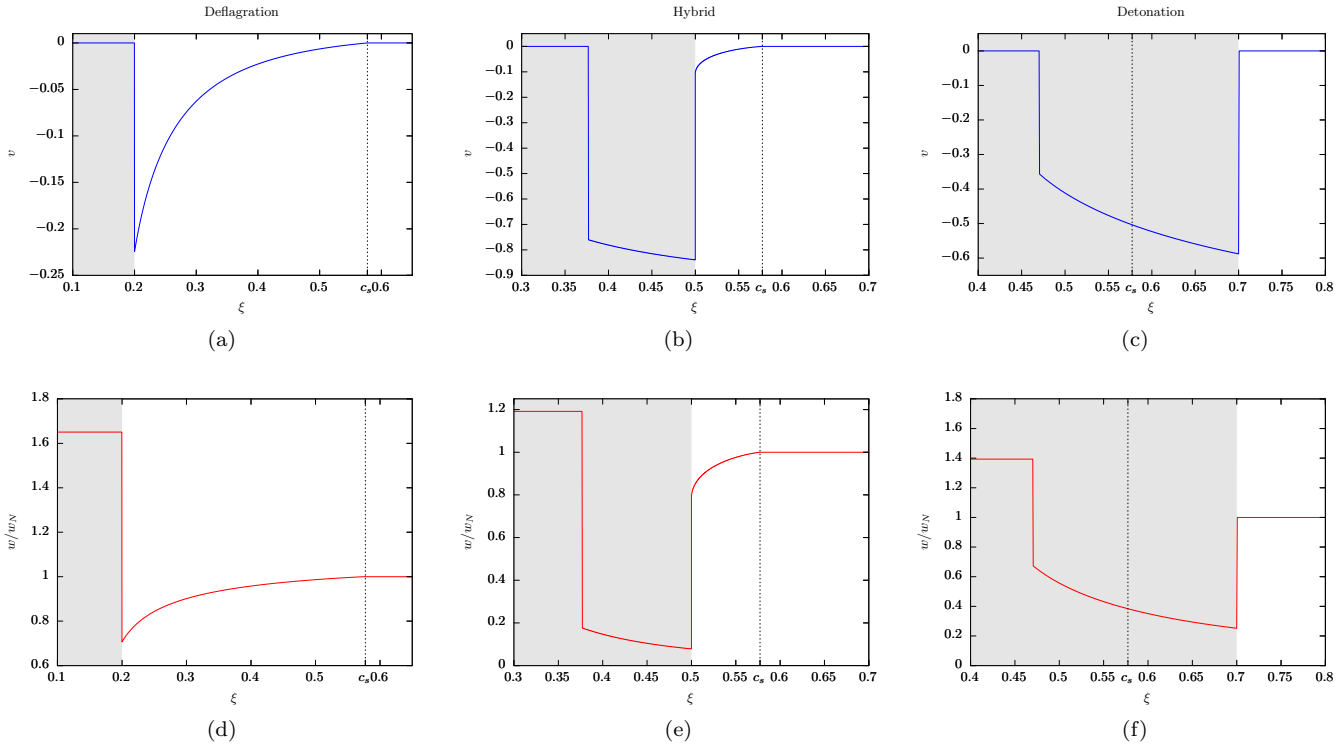

Figure 4. Velocity and enthalpy profiles for the three kind of solutions discussed. Subfigures 4a and 4d correspond to a deflagration with $v_w = 0.2$. Subfigures 4b and 4e correspond to a hybrid with $v_w = 0.5$. Subfigures 4c and 4f correspond to a detonation with $v_w = 0.7$.

V. EXPANSION REGIMES

In this section, we discuss the possible expansion regimes depending on the velocity of the bubble wall.

If $v_w < c_s$, we need to start with $v_- = 0$ behind the wall. This implies that, in the RF of the wall, $\tilde{v}_- = v_w$. To have $v_+ < 0$, it is necessary that $\tilde{v}_+ > \tilde{v}_-$. This means that the velocities just behind and in front of the wall both belong to the lower left region of Figure 3, with both velocities being subsonic. This kind of solutions are called deflagrations.

If $v_w > c_s$, it is required that we start with $v_+ = 0$ in front of the wall. So, in the RF of the wall, $\tilde{v}_+ = v_w$ in order to have the matter at rest outside of the bubble. To have negative velocities behind the wall, it is necessary that $\tilde{v}_- > \tilde{v}_+$. This implies that the velocities just behind and in front of the wall belong to the upper right region of Figure 3, which means that both velocities are subsonic. This solutions are called detonations.

It is possible to build an alternative profile that combines both a detonation and a deflagration. This is discussed in subsection V C.

A. Deflagrations ($v_w < c_s$)

This type of profile corresponds to the upper left area of Figure 1. To build these solutions, we start just behind the wall ($\xi_0 = v_w$), where $v_- = 0$. This means that $\tilde{v}_- = v_w$. Then we can find the values just in front of the wall solving the MC (setting an arbitrary value for w_-) which results in a value for $\tilde{v}_+$ and w_+. Computing the Lorentz transformed velocity v_+, we can evolve using the equations 4 and 5 until v reaches zero, which is a fixed point. Performing a shooting method algorithm to find the value of w_- that builds the desired profile is required to reach the value of $w = w_N$ outside the bubble.

It is not possible to have this profile for an arbitrary v_w with an arbitrary large ϵ. If we increase the value of ϵ for a certain value of v_w, the value of $\tilde{v}_+$ (and also v_+) will increase until the value of $\tilde{v}_+$ reaches c_s, from which there are not any physical solutions. This limit is represented with the dotted red line in Figures 1 and 3, where the shadowed part shows the inaccessible region.

Figures 4a and 4d show the computed profiles for a deflagration with $v_w = 0.2$ and $\epsilon/w_N = 0.16$. This profile resulted in $\alpha_+ = 0.31$ and $r = 2.34$.

B. Detonations ($v_w > c_s$)

This kind of solutions are the ones that begin on the right side of Figure 1. Starting from a point $\xi_0 > c_s$, there is no way to evolve the equation smoothly to $v = 0$. It necessarily means that a shock front connects the profile to zero inside the bubble. The position of this shock is determined by the point where we can solve the MC with $\epsilon = 0$ (as there is no phase transition) from the actual v_+

and w_+ to $v_- = 0$.

To build the solution, we start with $\xi_0 = v_w$, $v_+ = 0$ and $w_+ = w_N$. Transforming the velocities to the RF of the wall and solving the MC, we find v_- and w_- to evolve the profile until it reaches the shock, where we know that the profile can be connected with $v = 0$, keeping all conservation rules. Shock front line is showed in Figure 1 and 3 with a blue dashed line.

Figures 4c and 4f are the result of a detonation with $v_w = 0.7$ and $\epsilon/w_N = 0.1$. It resulted in $\alpha_+ = 0.14$ and $r = 0.25$.

C. Hybrids ($v_w < c_s$)

There exists another possibility of subsonic ($v_w < c_s$) solution that combines both profiles previously described. This hybrid profile behaves like the described deflagrations behind the wall and like the detonations in front of the wall. The profile inside the bubble is in the region between the green and the blue lines in Figure 1. If we tried to build a profile using the same procedure as for detonations, the MC through the wall would give us a non-physical profile. The reason is that setting $v_+ = 0$ in a region $\xi < c_s$ implies that $\tilde{v}_+ < c_s$ and the region that we are looking at has supersonic velocities in the local RF. The only way of building a profile in this region is that, in front of the wall the local velocity is $\tilde{v}_+ = c_s$, that is the lower limit for this velocity that respects the entropy conditions.

To build this solution we start with $\xi_0 = v_w \lesssim c_s$, to ensure that, behind the wall, the velocity is below (more negative) the line $\mu(\xi, v)\xi = c_s^2$. As we discussed, the only possible value for the velocity in front of the wall in the local RF is $\tilde{v}_+ = c_s$. We can solve the MC and get the velocity behind the wall, which will be in the region between the blue and the green line in Figure 1. We can evolve this condition until it reaches the shock, that will connect the profile to zero. On the other side of the wall, we have that $\tilde{v}_+ = c_s$, so in the RF of the centre of the bubble, the velocity will be on the red line in Figure 1. From this point, the profile can be evolved to zero smoothly, like a typical deflagration.

This kind of profile could not happen in the shadowed region of the Figure 1 because both sides of the wall would evolve in the same direction, so it is impossible to connect to $v = 0$ behind the wall.

Figures 4b and 4e show the profiles of this kind of solutions with $v_w = 0.5$ and $\epsilon/w_N = 0.07$. The solution obtained has $\alpha_+ = 0.095$ and $r = 0.077$.

VI. CONCLUSIONS

This work is the first one that studies the velocity and enthalpy profile of overheated relativistic bubbles in an astrophysical context. We have found three different kinds of solutions depending on the bubble wall velocity v_w and the self-interacting energy ϵ.

It can be seen that, in all the profiles, enthalpy decreases at the surroundings of the wall. This, together with the fact that $v < 0$, are consequences of the energy conservation and the equations of state that we have imposed, which require that the enthalpy inside the bubble is greater than outside.

The three regimes found are also present in the studies of overcooled bubbles but all of them have qualitative differences. The deflagration profiles found in this work present a rarefaction region in front of the wall that smoothly connects with the metastable state. In contrast, for overcooled bubbles, the deflagrations are preceded by a compression region which ends in a shock front. Complementary, for overheated bubbles, detonations are followed by a compression region that ends in a shock, while for overcooled bubbles there is a rarefaction region that smoothly connects with the interior of the bubble. Finally, in both situations there are hybrid solutions but, in contrast to overcooled bubbles these appear for subsonic wave fronts.

As we explained, this model could be representative of the bubble profiles nucleated in a NS merge.

ACKNOWLEDGMENTS

I want to thank specially my thesis advisor Dr. Jorge Casalderrey who has given me all the necessary support to write this work. I also want to thank my family, partner and friends, who have encouraged me throughout all the process of completing this thesis.

[1] José R. Espinosa, Thomas Konstandin, José M. No, and Géraldine Servant. Energy budget of cosmological first-order phase transitions. *Journal of Cosmology and Astroparticle Physics*, 2010(06):028, jun 2010.

[2] Mark Hindmarsh and Mulham Hijazi. Gravitational waves from first order cosmological phase transitions in the sound shell model. *Journal of Cosmology and Astroparticle Physics*, 2019(12):062, dec 2019.

[3] Mark Hindmarsh, Marvin Lüben, Johannes Lumma, and Martin Pauly. Phase transitions in the early universe. *SciPost Phys. Lect. Notes*, page 24, 2021.

[4] A. Tawfik and T. Harko. Quark-hadron phase transitions in the viscous early universe. *Phys. Rev. D*, 85:084032, Apr 2012.

[5] Jorge Casalderrey-Solana, David Mateos, and Mikel Sanchez-Garitaonandia. Mega-hertz gravitational waves from neutron star mergers. *arXiv preprint arXiv:2210.03171*, 2022.

[6] Lev Davidovich Landau and Evgenii Mikhailovich Lifshitz. *Fluid Mechanics: Landau and Lifshitz: Course of Theoretical Physics, Volume 6*, volume 6. Elsevier, 2013.